Linewidth of the harmonics in a microwave frequency comb generated by focusing a mode-locked ultrafast laser on a tunneling junction

Mark J. Hagmann, Frank S. Stenger, and Dmitry A. Yarotski

Citation: Journal of Applied Physics **114**, 223107 (2013); doi: 10.1063/1.4831952
View online: https://doi.org/10.1063/1.4831952
View Table of Contents: http://aip.scitation.org/toc/jap/114/22
Published by the American Institute of Physics

JOURNAL OF APPLIED PHYSICS **114**, 223107 (2013)

Linewidth of the harmonics in a microwave frequency comb generated by focusing a mode-locked ultrafast laser on a tunneling junction

Mark J. Hagmann,[1] Frank S. Stenger,[2] and Dmitry A. Yarotski[3]
[1]*Department of Electrical and Computer Engineering, University of Utah, Salt Lake City, Utah 84112, USA*
[2]*School of Computing, University of Utah, Salt Lake City, Utah 84112, USA*
[3]*Center for Integrated Nanotechnologies, Materials Physics and Applications Division, Los Alamos National Laboratory, Los Alamos, New Mexico 87545, USA*

(Received 9 May 2013; accepted 4 November 2013; published online 13 December 2013)

Previous analyses suggest that microwave frequency combs (MFCs) with harmonics having extremely narrow linewidths could be produced by photodetection with a mode-locked ultrafast laser. In the MFC generated by focusing a passively mode-locked ultrafast laser on a tunneling junction, 200 harmonics from 74.254 MHz to 14.85 GHz have reproducible measured linewidths approximating the 1 Hz resolution bandwidth (RBW) of the spectrum analyzer. However, in new measurements at a RBW of 0.1 Hz, the linewidths are distributed from 0.12 to 1.17 Hz. Measurements and analysis suggest that, because the laser is not stabilized, the stochastic drift in the pulse repetition rate is the cause for the distribution in measured linewidths. It appears that there are three cases in which the RBW is (1) greater than, (2) less than, or (3) comparable with the intrinsic linewidth. The measured spectra in the third class are stochastic and may show two or more peaks at a single harmonic.
[http://dx.doi.org/10.1063/1.4831952]

INTRODUCTION

Recently, it was shown that a microwave frequency comb (MFC) may be generated in the tunneling current of a scanning tunneling microscope (STM) by focusing a mode-locked ultrafast laser pulse on the tunneling junction.[1] Others have generated frequency combs using photodetectors[2] or photoconductive antennas[3] for applications in frequency[2] and distance[3] metrology, but this presentation appears to be the first step toward bringing this type of measurement to scanning probe microscopy (SPM). The harmonics of the MFC, at integer multiples of the pulse repetition frequency of the laser, were measured at frequencies up to 14.85 GHz (200th harmonic), each having a linewidth (full width at half maximum, FWHM) of less than 1 Hz.

Kartner *et al.*[4] considered the MFC comb produced by photodetection with a mode-locked laser, assuming that the timing jitter of the laser pulses has a much greater effect than the amplitude noise on the linewidths of the harmonics. Their analysis suggests that each harmonic is Lorentzian with a linewidth proportional to the square of the harmonic number. They concluded that with ideal stabilization of the laser, the microwave linewidth could be reduced to 10^{-17} Hz (approximately the reciprocal of the age of the Earth). Eliyahu *et al.*[5] considered the microwave spectrum from photodetection of a mode-locked laser pulse train where the timing of each pulse depends only on the previous pulse in a nonstationary process. Thus, a correlation time τ_C is defined over short time scales, but in general the average change in the pulse position is unbounded. They concluded that for $\tau_C \ll T$ (pulse repetition period), corresponding to the case studied by Kartner *et al.*,[4] at low frequencies each harmonic has a Lorentzian spectrum with a linewidth proportional to the square of the harmonic number. However, for $\tau_C \gg T$, Eliyahu *et al.*[5] predicted that each harmonic can either be Lorentzian or Gaussian, with a linewidth proportional to either the first or second power of the harmonic number, depending on the frequency and magnitude of the timing jitter.

Here, we derive expressions for the linewidth of the MFC harmonics generated by the intermodal mixing of ultrashort laser pulses focused on the tunneling junction of a STM. This derivation takes into account the effects of finite pulse train duration, due to limited acquisition time or the coherence length of the laser, in addition to the timing jitter. The analysis shows that in our measurements, the linewidth is limited by the resolution bandwidth of the detection instrument rather than by the generation process itself.

DERIVATION OF THE SPECTRUM FOR A MFC IN LASER-ASSISTED STM

When the applied DC bias potential V_0 is small, the DC tunneling current I_0 in a tunneling junction, such as a metal-insulator-metal (MIM) diode or a STM, is related to the bias by the following approximate expression:

$$I_0 = AV_0 + BV_0^2 + CV_0^3. \tag{1}$$

The coefficients A, B, and C depend on the materials of the two electrodes and their spacing, and both measurements with MIM diodes[6] and analysis[7,8] show that the quadratic term in Eq. (1) is negligible for low values of V_0.

When the radiation from a mode-locked ultrafast laser is focused on a tunneling junction, the electric field of the radiation effectively superimposes a time-varying potential on the applied DC bias V_0 because the junction is much smaller than the wavelength. Thus, assuming that each laser pulse is Gaussian, and the duration of the measured pulse train is limited by either the acquisition time or the coherence length of the laser to 2N + 1 pulses, the effective random process for the potential is given by

$$V(t) = V_0 + \sum_{n=-N}^{N} V_n e^{-\left(\frac{t-nT+\Theta_n}{\tau}\right)^2}\cos[\omega_0(t-nT+\Theta_n)]. \quad (2)$$

Here, ω_0 is the optical frequency, and we introduce the random variable Θ_n as the timing jitter (seconds) of the nth pulse. Assuming that the current-voltage characteristics of the tunneling junction are given by Eq. (1) for the laser radiation, and making the adiabatic approximation of neglecting all photon-induced processes, the following equation is obtained for the random process of the tunneling current, where the cross terms in the square and cube of the summations are neglected because $T \gg \tau$:

$$\begin{aligned} I(t) =& I_0 + \left(A + 2BV_0 + 3CV_0^2\right)\sum_{n=-N}^{N} V_n e^{-\left(\frac{t-nT+\Theta_n}{\tau}\right)^2} \\ &\times \cos[\omega_0(t-nT+\Theta_n)] \\ &+ (B+3CV_0)\sum_{n=-N}^{N} V_n^2 e^{-2\left(\frac{t-nT+\Theta_n}{\tau}\right)^2} \\ &\times \cos^2[\omega_0(t-nT+\Theta_n)] \\ &+ C\sum_{n=-N}^{N} V_n^3 e^{-3\left(\frac{t-nT+\Theta_n}{\tau}\right)^2}\cos^3[\omega_0(t-nT+\Theta_n)]. \quad (3) \end{aligned}$$

Equation (3) is simplified with trigonometric identities, and the terms at the laser frequency and its harmonics are deleted, to obtain an expression for the rectified current which is caused by the laser. Following Kartner *et al.*[4] and Eliyahu *et al.*,[5] we assume that timing jitter has a greater effect on the linewidth than the amplitude noise, so the variable V_n is replaced by the constant V_1, as the amplitude of the effective potential caused by each laser pulse. Thus, we obtain the following expression for the random process for the total tunneling current in the time domain:

$$I(t) = I_0 + \frac{(B+3CV_0)}{2}V_1^2 \sum_{n=-N}^{N} e^{-2\left(\frac{t-nT+\Theta_n}{\tau}\right)^2}. \quad (4)$$

The following expression for the random process of the Fourier transform of the rectified current is obtained, requiring a step to complete the square in the exponent:

$$I(\omega) = \sqrt{\frac{\pi}{2}}\frac{(B+3CV_0)\tau V_1^2}{2} e^{\frac{-\omega^2\tau^2}{8}} \sum_{n=-N}^{N} e^{-i\omega(nT-\Theta_n)}. \quad (5)$$

The direct Fourier approach, as defined by Peebles,[9] is used to determine the power spectral density (PSD) of the random process x(t) over the time interval [0,T′]

$$G(T',\omega) = \frac{|X(T',\omega)|^2 R_L}{T'}. \quad (6)$$

Here, $X(T',\omega)$ is the Fourier transform of x(t) evaluated over the interval [0,T′],[10] and R_L is the resistive load. Now, using the random process $I(\omega)$ from Eq. (5) with $T' = (2N+1)T$ leads to the following expression for the PSD:

$$\begin{aligned} G(T,\omega) =& \frac{\pi(B+3CV_0)^2\tau^2V_1^4R_L}{8(2N+1)T} e^{\frac{-\omega^2\tau^2}{4}} \\ &\times \sum_{n=-N}^{N} e^{-i\omega(nT-\Theta_n)} \sum_{n=-N}^{N} e^{+i\omega(nT-\Theta_n)}. \quad (7) \end{aligned}$$

Euler's identity is used to evaluate the exponentials in the two summations to give the following:

$$\begin{aligned} G(T,\omega) =& \frac{\pi(B+3CV_0)^2\tau^2V_1^4R_L}{8(2N+1)T} e^{\frac{-\omega^2\tau^2}{4}} \\ &\times \left[\left[\sum_{n=-N}^{N} \cos[\omega(nT-\Theta_n)]\right]^2 \right. \\ &\left. + \left[\sum_{n=-N}^{N} \sin[\omega(nT-\Theta_n)]\right]^2\right]. \quad (8) \end{aligned}$$

Finally, trigonometric identities are used to obtain the following expression for the PSD:

$$G(T,\omega) = \frac{\pi(B+3CV_0)^2\tau^2V_1^4R_L}{8(2N+1)T} e^{\frac{-\omega^2\tau^2}{4}} \left[\begin{array}{l} \left[\sum_{n=-N}^{N} \cos(n\omega T)\cos(\omega\Theta_n) + \sin(n\omega T)\sin(\omega\Theta_n)\right]^2 \\ + \left[\sum_{n=-N}^{N} \sin(n\omega T)\cos(\omega\Theta_n) - \cos(n\omega T)\sin(\omega\Theta_n)\right]^2 \end{array}\right]. \quad (9)$$

It is convenient to define a frequency offset δ/T from the Mth harmonic, so that within the interval $-1/2 < \delta < 1/2$ the frequency is given by the following expression:

$$f = \frac{M+\delta}{T}. \quad (10)$$

Thus, Eq. (9) may be written as follows to show the effects of the frequency offset:

$$G(T,\omega)=\frac{\pi(B+3CV_0)^2\tau^2V_1^4R_L}{8(2N+1)T}e^{-\left(\pi M\frac{\tau}{T}\right)^2}\left[\begin{array}{l}\left[\sum_{n=-N}^{N}\cos(2\pi n\delta)\cos(\omega\Theta_n)+\sin(2\pi n\delta)\sin(\omega\Theta_n)\right]^2\\+\left[\sum_{n=-N}^{N}\sin(2\pi n\delta)\cos(\omega\Theta_n)-\cos(2\pi n\delta)\sin(\omega\Theta_n)\right]^2\end{array}\right]. \quad (11)$$

Even with a deterministic expression for the PSD, there would be a non-zero linewidth because of the explicit use of a finite duration for the random process. Thus, to establish a basis for comparison, next the PSD for zero timing jitter is determined in Eqs. (12) to (14):

$$G(T,\omega)_{\Theta_n=0}=\frac{\pi(B+3CV_0)^2\tau^2V_1^4R_L}{8(2N+1)T}e^{-\left(\pi M\frac{\tau}{T}\right)^2}\times\left(\frac{\sin[(2N+1)\pi\delta]}{\sin(\pi\delta)}\right)^2. \quad (12)$$

Thus, for the case where there is no timing jitter, the linewidth (FWHM) of the Mth harmonic is given by $\gamma_0=2\delta_0/T$, where δ_0 is determined using the following expression:

$$\left(\frac{\sin[(2N+1)\pi\delta_0]}{(2N+1)\pi\delta_0}\right)^2=\frac{1}{2}. \quad (13)$$

Solving Eq. (13) iteratively shows that $(2N+1)\pi\delta_0 = 1.3915574$ rad, so the spectral FWHM of the Mth harmonic is given by

$$\gamma_0=\frac{0.88589294}{(2N+1)T.} \quad (14)$$

Equation (14) shows that to measure a linewidth of 10^{-17} Hz, which Kartner *et al.*[4] considered as the limit with an ideally stabilized laser, the acquisition time and the coherence length of the laser must both exceed 8.86×10^{16} s, which is approximately the age of the Earth. To accomplish this at a frequency of 1 GHz would require N to be at least 4.43×10^{25}.

In order to make approximations that are consistent with the conditions for our measurements, we determine approximate values of N for which our measured linewidths could be explained by the effects of the finite acquisition time. These must be lower bounds for the actual values of N because other effects including timing jitter are not included. Our measurements have been made using a spectrum analyzer at resolution bandwidths (RBW) of 1 Hz or 0.1 Hz, corresponding to acquisition times of 1.8 or 18 s, respectively. The mode-locked laser has a pulse repetition frequency of 74.254 MHz so that T = 13.467 ns, where the acquisition time is equal to (2N + 1)T. Thus, $N = 6.67\times10^7$ for an RBW of 1 Hz, and 6.67×10^8 for an RBW of 0.1 Hz. Note that Eq. (14) shows that, with no timing jitter, the measured linewidth would be 0.49 Hz with an RBW of 1 Hz, and 0.049 Hz with an RBW of 0.1 Hz, which are comparable to our measurements.

Exactly at the peak of the Mth harmonic, because $\omega_M\Theta_n \ll 1$, Eq. (11) shows that

$$G(T,\omega_M)=\frac{\pi(2N+1)(B+3CV_0)^2\tau^2V_1^4R_L}{8T}\times e^{-\left(\pi M\frac{\tau}{T}\right)^2}\left(1-\omega_M^2\Theta_{RMS}^2\right), \quad (15)$$

where Θ_{RMS} is the rms value of the timing jitter. Thus, the timing-jitter causes a small decrease in the power spectral density at the peak for the Mth harmonic, which is proportional to M^2, so this decrease is more prominent at the higher-order harmonics.

Next values that are typical for our measurements will be used to guide the approximations in determining the contribution of timing jitter to the linewidth. Equation (11) shows that, with timing jitter, the linewidth (FWHM) of the Mth harmonic be given by $\gamma_1=2\delta_1/T$, where the equation for δ_1 is as follows:

$$\left[\begin{array}{l}\left[\sum_{n=-N}^{N}\cos(2\pi n\delta_1)\cos(\omega\Theta_n)\right]^2+\left[\sum_{n=-N}^{N}\sin(2\pi n\delta_1)\sin(\omega\Theta_n)\right]^2\\+\left[\sum_{n=-N}^{N}\sin(2\pi n\delta_1)\cos(\omega\Theta_n)\right]^2+\left[\sum_{n=-N}^{N}\cos(2\pi n\delta_1)\sin(\omega\Theta_n)\right]^2\end{array}\right]=\frac{1}{2}\left[\sum_{n=-N}^{N}\cos(\omega\Theta_n)\right]^2. \quad (16)$$

Note that from Eq. (14), the argument $2\pi n\delta_1$ in Eq. (16) is approximately 0.4429 πn/N in the summations so no expansions are used for the functions of this argument. First, we expand the functions of $\omega\Theta_n$ in Eq. (16) to second order in this variable

$$\left[\begin{array}{l}\left[\sum_{n=-N}^{N}\cos(2\pi n\delta_1)\left(1-\frac{\omega^2\Theta_n^2}{2}\right)\right]^2+\left[\sum_{n=-N}^{N}\sin(2\pi n\delta_1)\omega\Theta_n\right]^2\\+\left[\sum_{n=-N}^{N}\sin(2\pi n\delta_1)\left(1-\frac{\omega^2\Theta_n^2}{2}\right)\right]^2+\left[\sum_{n=-N}^{N}\cos(2\pi n\delta_1)\omega\Theta_n\right]^2\end{array}\right]=\frac{1}{2}\left[\sum_{n=-N}^{N}\left(1-\frac{\omega^2\Theta_n^2}{2}\right)\right]^2. \quad (17)$$

Performing the squares in Eq. (17) and retaining the terms to second order

$$\left(\frac{\sin[(2N+1)\pi\delta_1]}{(2N+1)\sin(\pi\delta_1)}\right)^2 - \frac{1}{2} - \left(\frac{\sin[(2N+1)\pi\delta_1]}{(2N+1)\sin(\pi\delta_1)}\right) \times \frac{1}{(2N+1)}\sum_{n=-N}^{N}\omega^2\Theta_n^2\cos(2\pi n\delta_1) + \left[\frac{1}{(2N+1)}\sum_{n=-N}^{N}\omega\Theta_n\sin(2\pi n\delta_1)\right]^2 + \left[\frac{1}{(2N+1)}\sum_{n=-N}^{N}\omega\Theta_n\cos(2\pi n\delta_1)\right]^2 + \frac{1}{2(2N+1)}\sum_{n=-N}^{N}\omega^2\Theta_n^2 = 0. \quad (18)$$

Finally, deleting the summations with oscillatory terms, and thus of smaller magnitude, gives the following expression for δ_1:

$$\left(\frac{\sin[(2N+1)\pi\delta_1]}{(2N+1)\sin(\pi\delta_1)}\right)^2 = \frac{1-\omega_M^2\Theta_{RMS}^2}{2}. \quad (19)$$

Equation (19) differs from Eq. (13), showing that timing jitter causes a small increase in the linewidth, which is proportional to M^2, so this increase is more prominent at the higher-order harmonics. Table I gives values for the fractional decrease in the PSD at the peak and the increase in the linewidth caused by timing jitter which were calculated using Eqs. (15) and (19).

The effects of timing jitter in a mode-locked laser have been modeled as a random walk.[11] Practical limits to the drift in the pulse repetition frequency require a bounded random walk model so that for large values of the acquisition time, $T_A > T_0$, the rms value of the random variable Θ_n approaches a constant Θ_0. Thus, the rms value, Θ_{RMS} is given by the following expressions, where the limit Θ_0, the time constant T_0, and the parameter α depend on the particular mode locking system that is used with the laser.

$$\Theta_{RMS} = \alpha\sqrt{T_A} \quad \text{for } T_A < T_0, \quad (20A)$$

$$\Theta_{RMS} = \Theta_0 \quad \text{for } T_A > T_0. \quad (20B)$$

Thus, from Eqs. (19), (20A), and (20B),

$$\left(\frac{\sin[(2N+1)\pi\delta_2]}{(2N+1)\sin(\pi\delta_2)}\right)^2 = \frac{1-\omega_M^2\alpha^2 T_A}{2} \quad \text{for } T_A < T_0, \quad (21A)$$

TABLE I. Fractional decrease in the peak PSD and increase in the linewidth caused by timing jitter.

Frequency	Θ_{rms} (deg)	Peak PSD decrease	Linewidth increase
74.254 MHz	10^{-8}	0.663%	0.444%
74.254 MHz	10^{-9}	0.00663%	0.00444%
7.4254 GHz	10^{-10}	0.663%	0.444%
7.4254 GHz	10^{-11}	0.00663%	0.00444%

$$\left(\frac{\sin[(2N+1)\pi\delta_3]}{(2N+1)\sin(\pi\delta_3)}\right)^2 = \frac{1-\omega_M^2\Theta_0^2}{2} \quad \text{for } T_A > T_0. \quad (21B)$$

The value of γ_0, which is the linewidth with no timing jitter, was already determined in Eq. (14). It is convenient to define $\beta \equiv (2N+1)\pi\delta_0 = 1.3915574$ rad, and consider the following function of $(\beta+\Delta)$, where $\Delta \ll \beta$

$$\frac{\sin(\beta+\Delta)}{(\beta+\Delta)} \approx \frac{\sin(\beta)}{\beta}\left[1-\Delta\left[\frac{1}{\beta}-\cot(\beta)\right]\right] = \frac{1}{\sqrt{2}}(1-0.53743591\Delta). \quad (22)$$

Combining Eqs. (19) and (22) gives the following expression for the linewidth with timing jitter:

$$\gamma_1 = \gamma_0\left[1+1.3371256\left[1-\sqrt{1-\omega_M^2\Theta_{RMS}^2}\right]\right] \approx \gamma_0\left(1+0.66856278\omega_M^2\Theta_{RMS}^2\right). \quad (23)$$

Combining Eq. (22) with Eqs. (20A) and (20B) gives the following expressions for the linewidth when the timing jitter is modeled as a bounded random walk

$$\gamma_2 \approx \gamma_0\left(1+.66856278\omega_M^2\alpha^2 T_A\right) \quad \text{for } T_A < T_0, \quad (24A)$$

$$\gamma_3 \approx \gamma_0\left(1+.66856278\omega_M^2{\Theta_0}^2\right) \quad \text{for } T_A > T_0. \quad (24B)$$

Equations (24A) and (24B) show that the measured linewidth varies inversely with the acquisition time for small values of T_A, and then reaches a plateau, with the possibility of returning to the inverse dependence at large T_A if the laser is stabilized to reduce T_0. Nevertheless, It must be acknowledged that as the length of the pulse train of the laser and the observation time are increased, the measured linewidth cannot be made arbitrarily small because other phenomena would become more evident—particularly the fundamental limit which is caused by the spectral width of the laser beam.[12]

MEASUREMENTS OF THE MICROWAVE FREQUENCY COMB GENERATED WITH A PASSIVELY MODE-LOCKED LASER AND A SCANNING TUNNELING MICROSCOPE

We have previously generated a microwave frequency comb with more than 200 measurable harmonics by focusing a passively mode-locked ultrafast laser on the tunneling junction of a STM.[1] The mechanism for this effect may be understood because the laser radiation imposes a pulsed electric field on the tunneling junction and the non-linear current-voltage characteristics of this junction cause optical rectification. Thus, there is a sequence of short (≈15 fs) pulses in the tunneling current having a separation (13.5 ns) which constitutes a microwave frequency comb.

The 15-fs pulse train from a Kerr-lens passively mode-locked Ti:Sapphire laser (CompactPro, Femtolasers; $\hbar\omega = 1.55$ eV) having a nominal pulse repetition frequency of

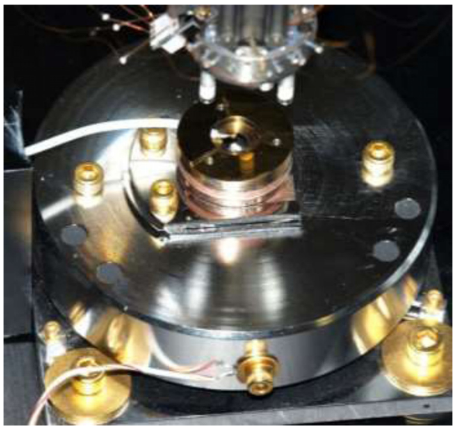

FIG. 1. STM measurement head showing the sample holder with a small gold bead as the sample at the end of a miniature coaxial cable.

74.254 MHz) was focused to a 100 μm spot at the tunneling junction of a scanning tunneling microscope (UHV700, RHK Technology) operated in air with a DC tunneling current of 10 μA. Freshly etched tungsten tips were annealed shortly before each measurement to remove water and oxide layers. The sample electrodes were small (dia. < 1 mm) beads of gold formed in a hydrogen flame. Figure 1 shows the STM measurement head with the sample holder and the gold bead which is connected to a section of miniature coaxial cable. Figure 2 is a block diagram of the apparatus, where a bias-T, represented by the capacitor and inductor, separates the bias supply from the microwave spectrum analyzer (RSA-6120B, Tektronix) in the sample circuit of the STM.

The laser was not stabilized, so thermal effects and vibrations caused the pulse repetition frequency to vary with time. The measured drift rate was typically 0.2 Hz/s, which corresponds to a change of 0.36 Hz or 3.6 Hz in the pulse repetition frequency during acquisition when using a RBW of 1 or 0.1 Hz, respectively. We have not yet made a full characterization of the timing jitter, but we have determined that step changes in the pulse repetition frequency occur as small "jumps" at irregular intervals. We have made measurements using a spectrum analyzer at RBWs of 1 Hz or 0.1 Hz, corresponding to acquisition times of 1.8 or 18 s, respectively, and the following data are consistent with our measurements of the timing jitter which show that the jumps in the pulse repetition frequency are more likely to occur during the longer acquisition time for a RBW of 0.1 Hz.

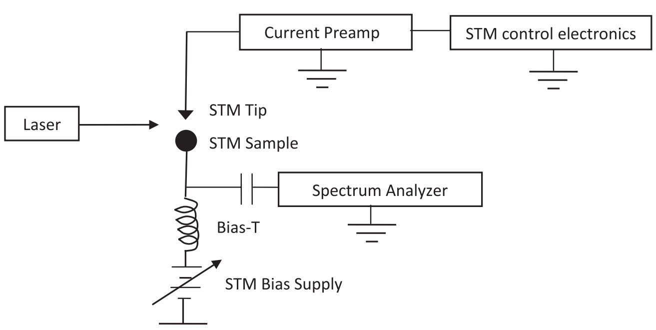

FIG. 2. Block diagram of apparatus to generate a microwave frequency comb by mixing in the tunneling junction of an STM.

TABLE II. Measurements with an RBW of 0.1 Hz.

File No.	Linewidth FWHM (Hz)	Peak power (dBm)
1	0.12	−138.72
2	0.14	−137.10
3	0.16	−141.47
4	0.16	−141.47
5	0.20	−151.28
6	0.23	−137.33
7	0.23	−142.47
8	1.17	−144.19

The linewidth for the fundamental of the microwave frequency comb, which is at the pulse repetition rate for the mode-locked laser (74.25 MHz), was measured using a RBW of 0.1 Hz, which is the lowest setting for the spectrum analyzer. Table II presents the measured linewidth and peak power for each of the eight measurements. This table shows that, with a RBW of 0.1 Hz, the linewidth varied by a factor of 9.8 and the peak power varied by 14 dB. However, much less variation has been seen in other measurements with a RBW of 1 Hz or greater. For example, using a RBW of 1 Hz with a different tip electrode, a set of six consecutive measurements of the peak power at the first harmonic had a mean of −121.83 dBm with a standard deviation of 0.47 dBm.

Figure 3 (File 1 of Table II) shows the power spectral density of the fundamental as a function of the frequency with a linewidth of 0.12 Hz. The solid squares represent the data measured by the spectrum analyzer and the dashed red curve is a best fit of these data using the dominant first term in the brackets of Eq. (13). The empirical value of $N = 2.62 \times 10^8$ corresponds to a pulse train having a duration of $(2N + 1)T = 7.06$ s, which is somewhat less than the acquisition time of 18 s when using a RBW of 0.1 Hz. The reduced value of the RBW in these measurements enables us to place a lower value for the upper bound of the linewidth than that found in the earlier measurements.[1]

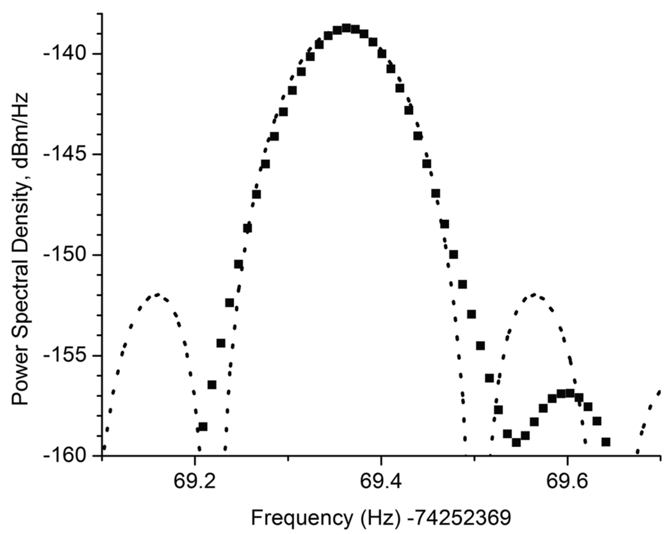

FIG. 3. Power spectral density in the fundamental at 74.25 MHz, with a linewidth of 0.12 Hz. Solid squares represent the measured data and the dashed red curve is a best fit using Eq. (13).

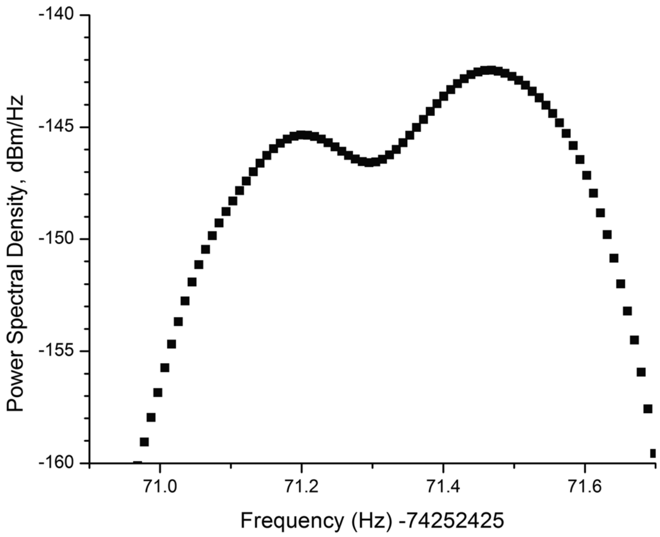

FIG. 4. Measured power spectral density in the fundamental at 74.25 MHz with a double peak having a total FWHM linewidth of 0.23 Hz.

Figure 4 (File 7 of Table II) shows the power spectral density of the fundamental as a function of the frequency for a double peak having a total linewidth of 0.23 Hz. The PSD at each peak is approximately one-half the value for the single peak in Fig. 3. Graphs for each of the 6 files having a linewidth greater than 0.14 Hz have two or more peaks in the PSD, whereas no measurements with more than one peak in the PSD were made earlier using a RBW of 1 Hz.[1] We attribute the presence of two or more peaks at a single harmonic to jumps in the pulse repetition frequency during the acquisition time.

DISCUSSION AND CONCLUSIONS

In any measurement of the spectrum of the harmonics in a microwave frequency comb, the apparent linewidth is limited by the effective length of the pulse train of the laser—which is the lesser of two values: the inherent length, and the duration of the measured sample. However, in our measurements the laser was not stabilized and we observe a drift in the pulse repetition frequency consisting of small "jumps" at irregular intervals. Thus, our measurements suggest that three separate cases may be defined:

(1) The RBW is much greater than the intrinsic linewidth. For example, with ideal stabilization of the laser, as considered by Kartner *et al.*,[4] the apparent linewidth would be equal to the RBW of the spectrum analyzer (e.g., 1 Hz with a RBW of 1 Hz, 0.1 Hz with a RBW of 0.1 Hz, etc.). We have made many measurements of the microwave frequency comb using a RBW of 1 Hz or 10 Hz, which show an apparent linewidth of approximately 1 Hz or 10 Hz, respectively, because there is a low probability for a jump in the pulse repetition frequency to occur during the corresponding short values of the acquisition time.

(2) The RBW is much less than the intrinsic linewidth. Spectrum analyzers with a RBW less than 0.1 Hz are not yet available. However, we anticipate that with such instruments the apparent linewidth would increase in proportion to the acquisition time up to the point where saturation would occur due to the finite bounds on the drift.

(3) The RBW is comparable with the intrinsic linewidth. In our measurements using the intermediate value of 0.1 Hz for the RBW, we observe a stochastic structure in the spectrum where 2 (e.g., Fig. 4) or rarely 3 peaks appear in the measured spectrum at a single harmonic of the microwave frequency comb, and attribute this to the occurrence of 1 or 2 jumps in the pulse repetition frequency during the acquisition time.

Some insight into these effects may be obtained by considering the present analysis using small values of N in the summations. Our calculations and measurements agree with previous work suggesting that timing jitter may be the dominant cause for the linewidth in a microwave frequency comb produced with an ultrafast laser.[4,5] However, it must be acknowledged that as the length of the pulse train of the laser and the observation time are increased, the measured linewidth could not be made arbitrarily small. This is because other sources would become more evident—particularly the fundamental limit caused by the spectral width of the laser beam.[12]

ACKNOWLEDGMENTS

This work was performed, in part, at the Center for Integrated Nanotechnologies, U.S. Department of Energy, Office of Basic Energy Sciences user facility. Los Alamos National Laboratory, an affirmative action equal opportunity employer, is operated by Los Alamos National Security, L.L.C., for the National Nuclear Security Administration of the U.S. Department of Energy under Contract No. DE-AC52-06NA25396. We also acknowledge support from the Department of Energy under Award No. DE-SC0006339.

[1]M. J. Hagmann, A. J. Taylor, and D. A. Yarotski, Appl. Phys. Lett. **101**, 241102 (2012).
[2]T. Yasui, S. Yokoyama, H. Inaba, K. Minoshima, T. Nagatsuma, and T. Araki, IEEE J. Sel. Top. Quantum Electron. **17**, 191 (2011).
[3]N. R. Doloca, M. Meiners-Hagen, M. Wedde, F. Pollinger and A. Abou-Zeid, Meas. Sci. Technol. **21**, 115302 (2010).
[4]F. X. Kartner, U. Morgner, T. Schibli, R. Ell, H. A. Haus, J. G. Fujimoto, and E. P. Ippen, "Few-cycle pulses directly from a laser," in *Few-Cycle Laser Pulse Generation and Its Applications*, Topics Appl. Phys. Vol. 95, edited by F. X. Kartner (Springer-Verlag, Berlin, Heidelberg, 2004), pp. 73–136.
[5]D. Eliyahu, R. A. Salvatore, and A. Yariv, J. Opt. Soc. Am. B **14**, 167 (1997).
[6]H. P. Knauss and R. A. Breslow, Proc. IRE **50**, 1843 (1962).
[7]J. G. Simmons, J. Appl. Phys. **34**, 238 (1963).
[8]J. G. Simmons, J. Appl. Phys. **34**, 1793 (1963).
[9]P. Z. Peebles, Jr., "Probability," in *Random Variables and Random Signal Principles* 3rd ed. (McGraw-Hill, New York, 1993), pp. 202–203.
[10]R. M. Howard, *Principles of Random Signal Analysis and Low Noise Design* (Wiley, New York, 2002), pp. 69–72.
[11]M. J. Ablowitz, B. Ilan, and S. T. Cundiff, Opt. Lett. **31**, 1875 (2006).
[12]N. Liu, Phys. Rev. A **47**, 4322 (1993).